This is a pre-peer reviewed version of the manuscript published in:

Electrochimica Acta, 2014, Volume 145, Pages 139-147

(DOI: 10.1016/j.electacta.2014.08.004)

Spectroelectrochemical study of the electrosynthesis of Pt nanoparticles/poly(3,4-(ethylenedioxythiophene) composite.

C. Fernandez-Blanco[1], D. Ibañez[1], A. Colina[1], V. Ruiz[2], A. Heras[1]*

1. Department of Chemistry, Universidad de Burgos, Pza. Misael Bañuelos s/n, E-09001 Burgos, Spain.
2. New Materials Division, IK4-CIDETEC, Paseo Miramón, 196 E-20009 Donostia - San Sebastián, Spain

* Corresponding author: Tel.: +34 947 258817; fax: +34 947 258831. E-mail address: maheras@ubu.es (A. Heras)

Abstract

UV-Visible, NIR and Raman spectroelectrochemistry techniques have been used for the *in-situ* study of Pt nanoparticles electrosynthesis on an electrochemically generated poly(3,4-ethylendioxythiophene) film. Two electrochemical steps have been necessary to obtain Pt nanoparticles with the appropriate size to be detected both by scanning electron microscopy and UV-Vis-NIR spectroelectrochemistry and with catalytic properties towards methanol oxidation. Changes in Raman spectra during the spectroelectrochemical synthesis and EDX analysis of the composites evidence that two steps are necessary for nanoparticle synthesis: 1) deposition of Pt nuclei on the polymer modified electrode, 2) growth of these nuclei to form nanoparticles yielding drastic changes in the spectroscopic signal and a significant increase of the amount of Pt.

Keywords: Conducting polymers, PEDOT, Platinum nanoparticles, Electrochemistry, Spectroelectrochemistry.

1. Introduction

Spectroelectrochemistry, a multiresponse technique that allows obtaining individual and complementary information about a complex system, has been successfully used to study multiple types of systems and reactions. Very different reaction mechanisms have been evaluated, providing insight into the reaction intermediates, the electrosynthesis of diverse materials or the behavior of a material towards a specific analyte [1–3]. In particular, UV-Visible-NIR and Raman spectroelectrochemistry have been proven to be very useful for studying the synthesis and for characterizing conducting polymers [4–7]. These types of polymers have been applied in different material science areas such as light emitting diodes, sensors and biosensors, solar cells or fuel cells [8–12]. In the case of fuel cells, modification of these polymers with suitable catalysts to improve the efficiency has been extensively studied [13–15]. Conducting polymers act as supporting material where the catalysts are anchored, allowing good dispersion and high stability. Most of these studies are mainly focused on characterizing the final product, not in understanding, and hence, optimizing the process towards a good final material. The most common techniques in these studies are electrochemistry, scanning electron microscopy (SEM) and some spectroscopic techniques [12–14,16–19], while the use of spectroelectrochemistry is comparatively more scarce.

Poly(3,4-ethylenedioxythiophene), PEDOT, is one of the most popular and widely used intrinsically conducting polymers (ICPs) due to its high conductivity, electrochemical stability, high transparency, catalytic ability and low band-gap [20–22]. Some ICPs, such as PEDOT, are ionic and electronic conductors, making them excellent and very efficient catalyst supports in hydrogen and methanol fuel cells [17,18,23,24]. Platinum is the most widespread catalyst used in direct methanol fuel

cells (DMFC) despite some drawbacks, such as poisoning during oxidation of methanol or the high cost of this metal. The use of Pt nanoparticles (PtNPs) is a typical strategy to decrease the amount of Pt in fuel cells and increase its efficiency.

To know how the polymer has been modified, it is usual to perform *ex-situ* analysis with, for example, electron microscopy techniques or some spectroscopies such as X-Ray Photoelectronic (XPS). Nevertheless, it is not widespread to carry out *in-situ* analysis to study the process of polymer modification and to characterize the modified polymer.

In this regard, the main objective of this work is to demonstrate that UV-Vis-NIR and Raman spectroelectrochemistry can help to follow the synthesis of a composite material consisting of poly(3,4-ethylendioxythiophene), PEDOT, and PtNPs with good electrocatalytic properties for methanol oxidation. Both components of the composite were electrochemically generated while the different steps of synthesis were followed with different *in-situ* spectroelectrochemical techniques to obtain valuable information about the process and the final product.

2. Experimental section

2.1. Materials

3,4-Ethylenedioxythiophene, EDOT (Aldrich), potassium hexachloroplatinate (IV), K_2PtCl_6 (Aldrich, >98%), lithium perchlorate trihydrate, $LiClO_4 \cdot 3\ H_2O$ (Panreac, >98%), perchloric acid, $HClO_4$ (Merk, 60%), and methanol (BDH Prolabo) were used as received. Aqueous solutions were prepared using high-quality water (resistivity of 18.2 MΩ·cm, Milli-Q A10 system, Millipore).

2.2. Microscopy measurements

Scanning Electron Microscopy (SEM) images were taken under high vacuum conditions with a JEOL JSM-6335F. Energy Dispersive X-Ray (EDX) spectra were recorded with the X-Ray spectrometer of a Scanning Electron Microscope JEOL JSM-6460LV.

2.3. Spectroelectrochemistry measurements

A standard three-electrode cell was used in all the experiments, consisting of a Pt wire auxiliary electrode, a homemade Ag/AgCl/KCl (3 M) microreference electrode and a 3 mm diameter glassy carbon (GC) disk working electrode (CHI Inc). Prior to electrosynthesis, the bare GC electrode was polished with alumina powder and then rinsed with ultrapure water in an ultrasonic bath for 30 min, changing the bath every 10 min.

UV-Visible spectroelectrochemical experiments were carried out in a cell described elsewhere [25] using a potentiostat PGSTAT 10 (Eco Chemie B.V.) coupled with a QE65000 Spectrometer (Ocean Optics) made up of a 1044x64 element diode array. The light beam, supplied by an Avalight DH-S deuterium-halogen light source (Avantes), was both conduced to and collected from the spectroelectrochemical cell by a 200 μm reflection probe (RP200-7-UV/Vis, Ocean Optics).

Near-infrared (NIR) spectroelectrochemical experiments were performed in the same cell arrangement [25], coupling in this case the potentiostat with a NIRQuest spectrometer (Ocean Optics) made up of a 512 pixels, covering the spectral range between 900 and 1700 nm. The light beam was supplied by the same light source indicated in the UV-Visible device and it was conducted to and collected

from the spectroelectrochemical cell by a 200 μm reflection probe (FCR-7IR200, Avantes).

In order to evaluate changes in UV-Vis and NIR spectra during the different steps of synthesis and characterization of the materials electrogenerated, reflectance changes referred to the film at the beginning of each experiment in the corresponding solution were plotted along the whole work.

Raman spectroelectrochemical experiments were carried out coupling the potentiostat to a Voyager Confocal Raman Spectrometer (BWTEK) using a laser source emitting at the wavelength of 532 nm and with a spectral resolution of 3.8 cm^{-1}. The measurements were performed with a 20x objective.

3. Results and discussion

Electrosynthesis of PtNPs/PEDOT composites was carried out in three consecutive steps, as described below. After some initial experiments in which the influence of different parameters was analyzed, such as EDOT or $PtCl_6^{2-}$ concentration, time and potential of polymerization, scan rate and vertex potentials for PtNPs deposition, the best experimental conditions for reproducibility in the electrosynthesis of this nanocomposite were achieved.

3.1. Electropolymerization of 3,4-ethylendioxythiophene (EDOT)

PEDOT films were electrosynthesized under potentiostatic conditions, applying +0.95 V for 10 s in a $3 \cdot 10^{-3}$ M EDOT and 0.30 M $LiClO_4$ aqueous solution (pH = 5) recording simultaneously whole spectra in the UV-Visible range. The chronoabsorptogram exhibits an ill-defined maximum around 590 nm and a broad band at wavelengths longer than 800 nm, characteristic of doped PEDOT (Fig 1a,

thick line). Experimental conditions selected to this electrosynthesis lead to generate a thin film just recovering the carbon electrode surface.

After electropolymerization, first the polymer was neutralized at -0.50 V for 20 s, registering simultaneously the UV-Visible spectra. Spectra evolution indicates that doped PEDOT was almost completely undoped during the first 2 s. Spectrum of neutral PEDOT film shows a characteristic maximum around 520 nm (Fig 1a, thin line). Next, the polymer film was stabilized in 0.3 M $LiClO_4$ aqueous solution by cycling the potential between -0.50 V and +0.70 V at 0.05 Vs^{-1}. Finally, it was tested the spectroelectrochemical behavior of PEDOT film in 0.50 M $HClO_4$ aqueous solution by cycling the potential between 0.00 V and +0.95 V at 0.025 Vs^{-1}. No significant changes were observed both in the voltammogram and in the spectral response, indicating that, probably due to the small thickness of the film no oligomers are retained during electrosynthesis of the film.

The electrosynthesis of the polymer was also studied with dynamic Raman spectroelectrochemistry [26], registering one Raman spectrum each second. Table 1 shows the main peaks registered corresponding to PEDOT undoped (column a) and doped state (column b) at -0.50 V and +0.95 V, respectively [27–31]. Temporal evolution of Raman spectra (Fig 1b) show the characteristic peaks of undoped PEDOT than of doped PEDOT, being the two most intense ones those at 1440 and 1523 cm^{-1}.

3.2. PtNPs electrosynthesis

Once PEDOT was electronsynthesized and spectroelectrochemically characterized, PtNPs were electrodeposited potentiodinamically on the top of the polymer film in two consecutive steps. Each of these steps consists of three

voltammetric cycles between -0.25 V and +1.00 V at 0.10 Vs^{-1} in $3 \cdot 10^{-3}$ M K_2PtCl_6 and 0.50 M $HClO_4$ aqueous solution (pH = 0.9). UV-Vis spectra have been recorded every 15 ms together with the cyclic voltammogram (CV). After this first set of three potential cycles (1^{st} step), the modified electrode was thoroughly washed with deionized water, the K_2PtCl_6 solution was changed and the 2^{nd} step of PtNPs synthesis was carried out.

During the 1^{st} step (3 first potential cycles) the voltammetric response (Fig 2, thin line) starts with the reduction of $PtCl_6^{2-}$ indicating that the first nuclei of Pt are being generated on the polymer-modified electrode surface. Although the first cycle is slightly different, the voltammogram reaches a stationary waveform in the next two ones. At +1.00 V Pt nuclei generated on the PEDOT film are oxidized. A small increase of the current intensity at this vertex potential with the number of cycles indicates that each cycle more Pt nuclei are electrodeposited in the cathodic potential region. These 3 first voltammetric cycles also exhibit a broad reduction peak around 0.00 V that decreases in intensity with the number of cycles. The limited information supplied by CVs makes difficult to understand all phenomena that are taking place during this 1^{st} step. Spectroscopic data obtained simultaneously provide valuable information related to the process, which would otherwise be inaccessible with *ex-situ* and tandem techniques.

Reflectance changes plotted versus wavelength (data not shown) present two different regions. At wavelengths shorter than 520 nm $\Delta R/R$ decreases during the forward scan and increases during the backward one. While at wavelengths longer than 520 nm the opposite behavior is observed.

Voltabsorptograms (VA) at two selected wavelengths, 450 and 900 nm, are shown in Fig 3. VA at 450 nm (Fig 3a, thin line) shows a linear decrease of

reflectance from -0.25 to +0.20 V in the three oxidation scans, followed by a stabilization of the signal until +0.80 V, where reflectance decreases again until +1.00 V is reached. Comparing this voltabsorptogram with that of the polymer in $HClO_4$ 0.50 M at the same wavelength (inset Fig 3a), it can be deduced that reflectance changes between -0.25 and +0.80 V are mainly due to oxidation of PEDOT film. However, the decrease of $\Delta R/R$ at 450 nm between +0.80 and +1.00 V observed for the polymer in Pt acid media and not appreciate in free-Pt acid media, must be due to oxidation of some Pt nuclei deposited on the film at the higher overpotential values. In the cathodic scans, there is a continuous linear increase of reflectance probably due to reduction of PEDOT film, but the initial value of reflectance is not recovered, as occurs in absence of Pt (inset Fig 3a). Trend is roughly the same in the three cycles, although a net but small decrease of reflectance is observed in consecutive cycles. Although these reflectance changes point out at oxidation and reduction processes related to $PtCl_6^{2-}$ anion and PEDOT film, there are not significant evidences to infer that NPs are generated on PEDOT film. The same conclusion can be extracted from VA at 900 nm (Fig 3b, thin line), although in this case reflectance increases during the anodic scans and decreases during the cathodic ones. Moreover, reflectance recovers the initial value after each cycle, although at +1.00 V it is observed a decrease of $\Delta R/R$ values of 20% cycle by cycle. Therefore, UV-Vis spectra registered during this 1st step of PtNPs synthesis supply not conclusive but interesting information related to oxidation of Pt species deposited on the PEDOT film although not to reduction of the $PtCl_6^{2-}$ anion.

Similar conclusions can be obtained from spectra registered in the NIR region during scans between -0.25 and +1.00 V at 0.10 Vs^{-1} in $3 \cdot 10^{-3}$ M K_2PtCl_6 and 0.50 M $HClO_4$ aqueous solution (pH = 0.9). Fig 4 (thin lines) illustrates the similarity

between the three spectra at -0.25 V during this first step of PtNPs synthesis. In view of the small spectral changes observed, we could assume that some Pt nuclei are formed, but only a slight modification of the film has taken place.

The same experimental procedure was used in the 2nd step of PtNPs electrosynthesis. Three potential cycles between -0.25 V and +1.00 V at 0.10 Vs^{-1} in $3 \cdot 10^{-3}$ M K_2PtCl_6 and 0.50 M $HClO_4$ aqueous solution (pH = 0.9) were carried out. Changes in voltammetric response (Fig 2, thick line) point out at more significant changes occurring on the polymer surface. First scan begins with a fast reduction of $PtCl_6^{2-}$, similar to that observed in the CV of the first step, followed by a nucleation peak at -0.18 V. This peak, not observed in the 1st step, should be related to reduction of Pt on the seeds generated in the previous step. During the reverse scan a sharp peak of reduction is also observed approximately at the same potential, -0.17 V. This peak could be related to the same process described before or to the reduction of protons adsorbed on the generated PtNPs. In the following scans, during the anodic scans the nucleation peak becomes less marked, while the reduction peak in the cathodic scans is slightly shifted to less negative potentials, -0.16 and -0.14 V for the second and third scan respectively. It is worth noting that the cathodic current does not increase with the number of potential cycles, which renders little information about PtNPs generation [17]. Furthermore, there are ill-defined peaks related to the adsorption-desorption of hydrogen on PtNPs, which could imply either that PtNPs are not generated or that they are well dispersed in PEDOT matrix [32]. Differences noted between CVs corresponding to the first and second steps of synthesis (Fig 2) support the second hypothesis, a good dispersion of the electrosynthesized nanoparticles, but again it is not possible to extract unambiguous conclusions only from electrochemical responses.

In the spectroscopic signals in Figure 3 (thick lines), more notable changes are observed in this second synthesis step. VA at 450 nm (Fig 3a, thick line) shows a similar trend to that observed for the first synthesis step from 0.00 V to +1.00 V, with a more pronounced decrease of reflectance during the anodic scan at potential higher than +0.85 V, and a linear increase of reflectance during the cathodic scan. Significant differences are observed at potentials lower than 0.00 V not appreciated in the 1st step. There is a small decrease of reflectance at potentials lower than -0.18 V at the end of the first potential cycle. This decrease of reflectance observed in this first potential cycle is significantly higher during the second and third scan starting also at potentials higher than -0.18 V (-0.14 V and -0.05 V for the second and third anodic scans, respectively). Similar behavior is observed in the voltabsorptogram at 900 nm (Fig 3b, thick line). A significant decrease of reflectance at potentials lower than -0.16 V occurs at the end of the first cathodic scan, while at the beginning of the second anodic one a constant reflectance value is kept until reaching -0.15 V. During the following scans, the trend is approximately the same, being the only difference the potential at which reflectance starts to decrease, around -0.13 V for the two last scans. The way the light is reflected on the electrode surface depends on the species adsorbed or deposited on it. Although PtNPs does not have a characteristic spectrum in UV-Vis region, these reflectance changes observed have to be related to PtNPs generation on the WE surface, considering that take place at potentials where voltammetrically it is observed the reduction of Pt anion. All these changes are also linked with changes in NIR spectra registered during this second electrosynthesis step. In this case, it is in the second and third scans where a clear decrease of reflectance is noticed from 900 to 1400 nm (Fig 4, thick lines).

Raman measurements supply direct information of how a surface is modified. For this reason, evolution of Raman spectra is recorded, trying to follow *in-situ* changes of PEDOT film during electrodeposition of Pt on its surface. Dynamic Raman spectroelectrochemistry experiments were performed taking one complete spectrum between 375 and 3000 cm^{-1} each second. These spectra revealed distinct features related to modification of the polymer film. Comparing pristine PEDOT film with modified PEDOT film after 1st PtNPs step of synthesis, Raman spectra at +0.95 V depicts, for the main peaks, negligible changes in peak position (Table 1, column b and c) but significant variations of peak intensity (Fig 5a). Plotting Raman intensity *vs.* potential at 1440 cm^{-1}, these changes are better understood (Fig 5b, thin lines). Raman signal decreases between 0.00 and +0.60 V where the polymer is been oxidized, reaching a practically constant value at potentials higher than +0.60 V where PEDOT is completely oxidized. However, between -0.25 and 0.00 V Raman intensity at 1440 cm^{-1} increases. This small potential window coincides with the region in which changes related to $PtCl_6^{2-}$ reduction in CV (Fig 2) and in UV-Vis voltabsorptograms (Fig 3) are also observed. Therefore, Raman changes produced between -0.25 and 0.00 V have to be due to PtNPs generation. While UV-Vis and NIR spectroscopies do not provide obvious evidences of Pt deposition in the 1st synthesis step, dynamic Raman spectroelectrochemistry indicates that the process occurs. Specifically, all PEDOT Raman peaks decreased a 50% in intensity , with the most pronounced changes occurring between 1400 and 1650 cm^{-1}, revealing that Pt species deposited on PEDOT film interact more intensively with the C_α=C_β and C_β-C_β chemical bonds. Even more dramatic changes were observed during the second step of PtNPs synthesis (Fig 5a) where the Raman intensity at 1440 cm^{-1} almost disappears (Fig 5b, thick line). From the behavior described for Raman signals, it can

be conclude that Pt has been electrodeposited on the PEDOT film, modifying and just weakening the vibration modes of the polymer film.

Summarizing information from cyclic voltammograms, VA at 450 and 900 nm, and NIR spectra, it is possible to conclude that PtNPs have been deposited on the PEDOT film after this 2nd synthesis step. PtNPs induce some changes in all these signals at potentials lower than 0.00 V, where $PtCl_6^{2-}$ is reduced, especially in Raman signals. Moreover, Raman spectra help to understand how deposited PtNPs interacts with PEDOT.

3.3. PtNPs/PEDOT composite characterization

To confirm the conclusions extracted from the spectroelectrochemical data, PtNPs/PEDOT composite films were characterized by scanning electron microscopy (SEM), also performing EDX analysis of the films, after the first and second synthesis steps (Fig 6).

SEM images of the composite material adsorbed on the electrode surface after the first three cycles of $PtCl_6^{2-}$ reduction does not evidence the presence of Pt on the PEDOT film, at the best resolution where the image can be obtained without damaging the polymer (Fig 6a). However, EDX analysis indicates that the film contains a 1.5% of Pt indicating that reduction has taken place as was deduced from Raman spectroelectrochemistry data. This SEM image also shows that the polymer layer adsorbed on the electrode is a very homogeneous film. SEM image of the film after the second synthesis step highlights the presence of homogeneous PtNPs of two different sizes (Fig 6b). The largest NPs have an average 98.2 ± 5.8 nm diameter while the smallest and more abundant ones have an average 29.5 ± 2.5 nm diameter. In addition, EDX analysis of the final material denotes that a 4.3% of Pt is

deposited on the PEDOT film. The amount of Pt after this 2nd step of synthesis is practically three times higher than that registered after the 1st step, indicating that the highest efficiency of PtNPs generation is achieved once small seeds of Pt are deposited on the polymer film. Therefore, spectral changes measured between -0.25 and 0.00 V by UV-Vis, NIR and Raman spectroelectrochemistry are clearly related to the generation and growth of these PtNPs observed in SEM images.

With these set of experiments it has been demonstrated that *in-situ* spectroelectrochemical measurements can help to obtain information about how the polymer surface has been modified. The electrochemical activity of the final PtNPs/PEDOT composite was evaluated by voltammetry in a 0.50 M $HClO_4$ (pH = 0.8) solution (Fig 7) between -0.235 and +0.85 V at 1.00 Vs^{-1}.Voltammogram reveals the characteristic features of polycrystalline Pt showing the hydrogen adsorption/desorption region and the Pt oxide formation/reduction region [33]. The increase of anodic current around +0.75 V is due to the oxygen adsorption while the reduction peak at +0.50 V corresponds to reduction of Pt oxide formed during the forward scan. Meanwhile, the two pairs of peaks between +0.05 and -0.20 V are attributed to adsorption/desorption of hydrogen atoms on the Pt surface. The pair of peaks at the lowest potentials around -0.10 V is due to weakly adsorbed hydrogen, while the other pair of peaks around 0.00 V is related to strongly adsorbed hydrogen [17,18,32]. The voltammogram proves that PtNPs deposited on PEDOT film are electrochemically active.

3.4. Methanol electro-oxidation

Finally, the catalytic activity of the PtNPs/PEDOT composite was tested by cycling it from 0.00 to +0.95 V at 0.025 Vs^{-1} in 2 M methanol and 0.50 M $HClO_4$ (pH = 0.8) solution. CV corresponding to the film after the first step of PtNPs

electrosynthesis (inset Fig 8) does not show methanol oxidation. This can be due either to insufficient amount of Pt or inadequate particle size of Pt nuclei generated on PEDOT film. However, CV for the composite obtained after the 2nd synthesis step displays the typical oxidation peaks of methanol (Fig 8, thin line). Figure 8 compares the catalytic response towards methanol oxidation of the composite proposed in this work with that of a massive Pt electrode. Two oxidation peaks were observed in both cases. The oxidation peak in the forward scan (I_p^f) is attributed to methanol oxidation, while the oxidation peak observed in the backward scan (I_p^b) is ascribed to carbonaceous intermediate species formed during the forward one [34–37]. The composite PtNPs/PEDOT exhibits lower peak potentials, E_p^f = +0.64 V and E_p^b = +0.55 V, than the bulk platinum electrode. On the other hand, the composite also shows a lower onset potential, +0.25 V for PtNPs/PEDOT compared to +0.35 V for the Pt electrode. Both values indicate that the composite reduce the overpotential for methanol oxidation more than a commercial Pt sheet.

4. Conclusions

A PtNPs/PEDOT composite has been successfully prepared by electrochemical techniques. The electrosynthesis process has been followed using *in-situ* spectroscopic techniques. UV-Visible and NIR spectroelectrochemistry data indicate that two deposition steps were necessary to obtain a polymer modified with PtNPs, as it was also corroborated by SEM and EDX. In addition, dynamic Raman spectroelectrochemistry revealed that PtNPs were not only deposited in the 2nd step but also some Pt species were formed in the first one. Pt particles generated both during the 1st and during the 2nd step were able to alter the vibrational modes of the PEDOT film, as noted by Raman spectroelectrochemistry. Furthermore, the

composite was interrogated for methanol oxidation, showing better electrocatalytic efficiency than a bulk Pt electrode.

After this work, it is possible to conclude that spectroelectrochemistry supplies important and definitive information related to processes in which the electrode surface is modified without performing *ex-situ* measurements. This information is obtained *in-situ* during the surface modification steps, being very direct and fast, which makes easier the characterization of a particular surface or material. Of course, *ex-situ* techniques are necessary to confirm this analysis, but it can be performed once a good reproducibility is achieved and the material shows the properties the researcher is looking for.

Acknowledgments

Support from Ministerio de Ciencia y Tecnología (CTQ2010-17127, V.R. Programa Ramón y Cajal), Junta de Castilla y León (GR71, BU349-U13), and Academy of Finland (V.R., Academy Research Fellow) is gratefully acknowledged. C. F-B. thanks Ministerio de Educación, Cultura y Deporte for a predoctoral FPU fellowship. D.I. is grateful for his FPI-MICINN agreement of the Ministerio de Economía y Competitividad. ICTS of Complutense University of Madrid (Spain) and PCT-UBU of Burgos University (Spain) are also acknowledged for electron microscope images and EDX analysis, respectively.

References

[1] V. Balland, M. Byrdin, A.P.M. Eker, M. Ahmad, K. Brettel, What makes the difference between a cryptochrome and DNA photolyase? A spectroelectrochemical comparison of the flavin redox transitions., J. Am. Chem. Soc. 131 (2009) 426–427.

[2] H. Shim, I. Yeo, S. Park, Simultaneous Multimode Experiments for Studies of Electrochemical Reaction Mechanisms: Demostration of Concept, Anal. Chem. 74 (2002) 3540–3546.

[3] N. Gonzalez-Dieguez, A. Colina, J. Lopez-Palacios, A. Heras, Spectroelectrochemistry at screen-printed electrodes: determination of dopamine, Anal. Chem. 84 (2012) 9146–9153.

[4] Y. Pang, X. Li, H. Ding, G. Shi, L. Jin, Electropolymerization of high quality electrochromic poly(3-alkyl-thiophene)s via a room temperature ionic liquid, Electrochim. Acta. 52 (2007) 6172–6177.

[5] L. Pigani, A. Heras, A. Colina, R. Seeber, J. Lopez-Palacios, Electropolymerisation of 3,4-ethylenedioxythiophene in aqueous solutions, Electrochem. Commun. 6 (2004) 1192–1198.

[6] G. Sonmez, H.B. Sonmez, C.K.F. Shen, F. Wudl, Red, Green, and Blue Colors in Polymeric Electrochromics, Adv. Mater. 16 (2004) 1905–1908.

[7] G. Sonmez, H.B. Sonmez, C.K.F. Shen, R.W. Jost, Y. Rubin, F. Wudl, A Processable Green Polymeric Electrochromic, Macromolecules. 38 (2005) 669–675.

[8] G. Gustafsson, Y. Cao, G.M. Treacy, F. Klavetter, N. Colaneri, A.J. Heeger, Flexible light-emitting diodes made from soluble conducting polymers, Nature. 357 (1992) 477–479.

[9] A. Ramanavicius, A. Ramanaviciene, A. Malinauskas, Electrochemical sensors based on conducting polymer-polypyrrole, Electrochim. Acta. 51 (2006) 6025–6037.

[10] U. Lange, N. V Roznyatovskaya, V.M. Mirsky, Conducting polymers in chemical sensors and arrays, Anal. Chim. Acta. 614 (2008) 1–26.

[11] A.F. Nogueira, C. Longo, M.A. De Paoli, Polymers in dye sensitized solar cells: overview and perspectives, Coord. Chem. Rev. 248 (2004) 1455–1468.

[12] G. Wu, K.L. More, C.M. Johnston, P. Zelenay, High-performance electrocatalysts for oxygen reduction derived from polyaniline, iron, and cobalt, Science. 332 (2011) 443–447.

[13] V. Selvaraj, M. Alagar, Pt and Pt–Ru nanoparticles decorated polypyrrole/multiwalled carbon nanotubes and their catalytic activity towards methanol oxidation, Electrochem. Commun. 9 (2007) 1145–1153.

[14] A. Lima, C. Coutanceau, J.M. Leger, C. Lamy, Investigation of ternary catalysts for methanol electrooxidation, J. Appl. Electrochem. 31 (2001) 379–386.

[15] B. Winther-Jensen, O. Winther-Jensen, M. Forsyth, D.R. Macfarlane, High rates of oxygen reduction over a vapor phase-polymerized PEDOT electrode., Science. 321 (2008) 671–674.

[16] J.-F. Drillet, R. Dittmeyer, K. Jüttner, L. Li, K.-M. Mangold, New Composite DMFC Anode with PEDOT as a Mixed Conductor and Catalyst Support, Fuel Cells. 6 (2006) 432–438.

[17] C.-W. Kuo, L.-M. Huang, T.-C. Wen, A. Gopalan, Enhanced electrocatalytic performance for methanol oxidation of a novel Pt-dispersed poly(3,4-ethylenedioxythiophene)-poly(styrene sulfonic acid) electrode, J. Power Sources. 160 (2006) 65–72.

[18] S. Patra, N. Munichandraiah, Electrooxidation of methanol on Pt-modified conductive polymer PEDOT, Langmuir. 25 (2009) 1732–1738.

[19] H. V. Patten, E. Ventosa, A. Colina, V. Ruiz, J. Lopez-Palacios, A.J. Wain, S.C.S. Lai, J.V. Macpherson, P.R. Unwin, Influence of ultrathin poly-(3,4-

ethylenedioxythiophene) (PEDOT) film supports on the electrodeposition and electrocatalytic activity of discrete platinum nanoparticles, J. Solid State Electrochem. 15 (2011) 2331–2339.

[20] L. Groenendaal, G. Zotti, P.-H. Aubert, S.M. Waybright, J.R. Reynolds, Electrochemistry of Poly(3,4-alkylenedioxythiophene) Derivatives, Adv. Mater. 15 (2003) 855–879.

[21] M. Lefebvre, Z. Qi, D. Rana, P.G. Pickup, Chemical Synthesis, Characterization, and Electrochemical Studies of Poly(3,4-ethylendioxythiophene)/poly(styrene-4-sulfonate) Composites, Chem. Mater. 11 (1999) 262–268.

[22] W. Feng, Y. Li, J. Wu, H. Noda, A. Fujii, M. Ozaki, K. Yoshino, Improved electrical and optical properties of Poly(3,4-ethylenedioxythiophene) via ordered microstructure, J. Phys. Condens. Matter. 19 (2007) 186220.

[23] C.-W. Kuo, C. Sivakumar, T.-C. Wen, Nanoparticles of Pt/HxMoO3 electrodeposited in poly(3,4-ethylenedioxythiophene)-poly(styrene sulfonic acid) as the electrocatalyst for methanol oxidation, J. Power Sources. 185 (2008) 807–814.

[24] C. Arbizzani, M. Biso, E. Manferrari, M. Mastragostino, Methanol oxidation by pEDOT-pSS/PtRu in DMFC, J. Power Sources. 178 (2008) 584–590.

[25] B. Zanfrognini, A. Colina, A. Heras, C. Zanardi, R. Seeber, J. Lopez-Palacios, A UV–Visible/Raman spectroelectrochemical study of the stability of poly(3,4-ethylendioxythiophene) films, Polym. Degrad. Stab. 96 (2011) 2112–2119.

[26] D. Ibañez, E.C. Romero, A. Heras, A. Colina, Dynamic Raman Spectroelectrochemistry of Single Walled Carbon Nanotubes modified electrodes using a Langmuir-Schaefer method, Electrochim. Acta. 129 (2014) 171–176.

[27] Z.-Q. Feng, J. Wu, W. Cho, M.K. Leach, E.W. Franz, Y.I. Naim, Z.Z. Gu, J.M. Corey, D.C. Martin, Highly aligned poly(3,4-ethylene dioxythiophene) (PEDOT) nano- and microscale fibers and tubes, Polymer. 54 (2013) 702–708.

[28] S. Garreau, G. Louarn, J.P. Buisson, G. Froyer, S. Lefrant, In Situ Spectroelectrochemical Raman Studies of Poly(3,4-ethylenedioxythiophene) (PEDT), Macromolecules. 32 (1999) 6807–6812.

[29] S. Garreau, G. Louarn, G. Froyer, M. Lapkowski, O. Chauvet, Spectroelectrochemical studies of the C14-alkyl derivative of poly(3,4-ethylenedioxythiophene) (PEDT), Electrochim. Acta. 46 (2001) 1207 – 1214.

[30] F. Tran-Van, S. Garreau, G. Louarn, G. Froyer, C. Chevrot, Fully undoped and soluble oligo(3,4-ethylenedioxythiophene)s: spectroscopic study and electrochemical characterization, J. Mater. Chem. 11 (2001) 1378–1382.

[31] M. Lapkowski, A. Pron, Electrochemical oxidation of poly(3,4-ethylenedioxythiophene) - “in situ” conductivity and spectroscopic investigations, Synth. Met. 110 (2000) 79–83.

[32] L. Niu, Q. Li, F. Wei, S. Wu, P. Liu, X. Cao, Electrocatalytic behavior of Pt-modified polyaniline electrode for methanol oxidation: Effect of Pt deposition modes, J. Electroanal. Chem. 578 (2005) 331–337.

[33] A.J. Bard, L.R. Faulkner, Electrochemical Methods. Fundamentals and Applications., 2nd ed., John Wiley & Sons, New York, 2001.

[34] Y. Chen, G. Zhang, J. Ma, Y. Zhou, Y. Tang, T. Lu, Electro-oxidation of methanol at the different carbon materials supported Pt nano-particles, Int. J. Hydrogen Energy. 35 (2010) 10109–10117.

[35] Z. Liu, X.Y. Ling, X. Su, J.Y. Lee, Carbon-Supported Pt and PtRu Nanoparticles as Catalysts for a Direct Methanol Fuel Cell, J. Phys. Chem. B. 108 (2004) 8234–8240.

[36] S. Sun, G. Zhang, N. Gauquelin, N. Chen, J. Zhou, S. Yang, W. Chin, X. Meng, D. Geng, M.N. Banis, R. Li, S. Ye, S. Knights, G.A. Botton, T.K. Sham, X. Sun, Single-atom catalysis using Pt/graphene achieved through atomic layer deposition, Sci. Rep. 3 (2013) 1775.

[37] Y. Zhao, L. Fan, H. Zhong, Y. Li, S. Yang, Platinum Nanoparticle Clusters Immobilized on Multiwalled Carbon Nanotubes: Electrodeposition and Enhanced Electrocatalytic Activity for Methanol Oxidation, Adv. Funct. Mater. 17 (2007) 1537–1541.

Captions to figures

Fig. 1. (a) UV-Vis spectra of PEDOT film at +0.95 V (blue thick line) and -0.50 V (red thin line). (b) Temporal evolution of Raman spectra during PEDOT synthesis at +0.95 V and its neutralization at -0.50 V.

Fig. 2. Cyclic voltammograms registered during the first (blue thick line) and second (red thin line) electrodeposition steps.

Fig. 3. (a) Voltabsorptograms at 450 nm during the first (blue thin line) and second (red thick line) electrodeposition steps. (b) Voltabsorptograms at 900 nm during the first (blue thin line) and second (red thick line) electrodeposition steps. $C_{K2PtCl6}$ = $3 \cdot 10^{-3}$ M; C_{HClO4} = 0.50 M. (Insets in both figures are voltabsorptograms at 450 and 900 nm of PEDOT film in $HClO_4$ 0.50 M.)

Fig. 4. NIR spectra at -0.25 V after each potential cycle during PtNPs electrosynthesis: first (blue thin lines) and second electrodeposition (red thick lines) step.

Fig. 5. (a) Raman spectra of PEDOT film (blue thick line), of PtNPs/PEDOT film during the 1st step of NPs synthesis (green thick line), and PtNPs/PEDOT film during the 2nd step of NPs synthesis (orange thin line) at +0.95 V. (b) Raman intensity *vs.* potential at 1440 cm^{-1} during the 1st (blue thin line) and 2nd (red thinck line) step of PtNPs synthesis; (● and ■ denotes the first point in each experiment).

Fig. 6. SEM images after the first (a) and second (b) synthesis step of PtNPs.

Fig. 7. Cyclic voltammogram of PtNPs/PEDOT composite in acid.

Fig. 8. Cyclic voltammograms of PtNPs/PEDOT composite during oxidation of methanol after the first (inset, green line) and second (magenta thin line) step of PtNPs. Cyclic voltammogram of bulk platinum electrode (blue thick line).

Fig1A

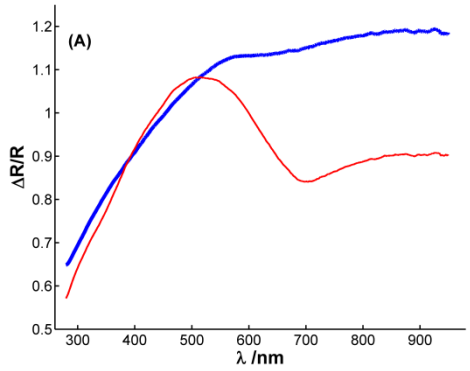

Fig1B

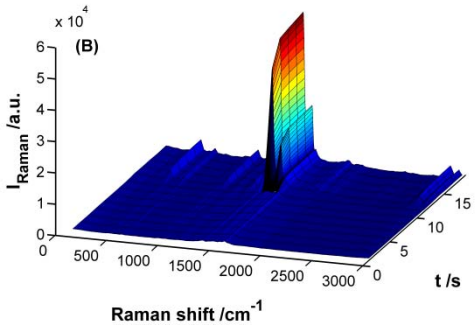

Fig2

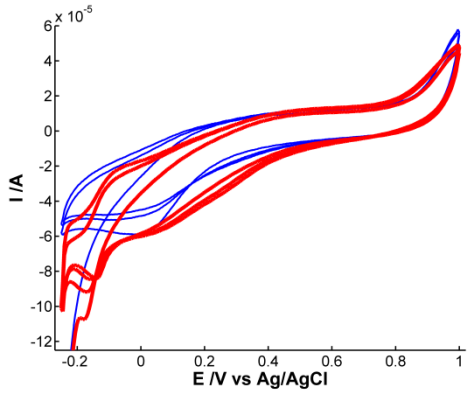

Fig3A

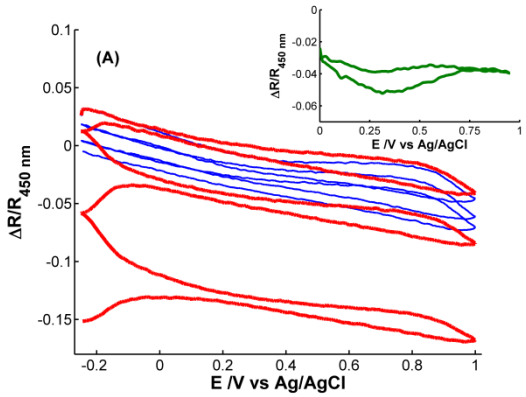

Fig3B

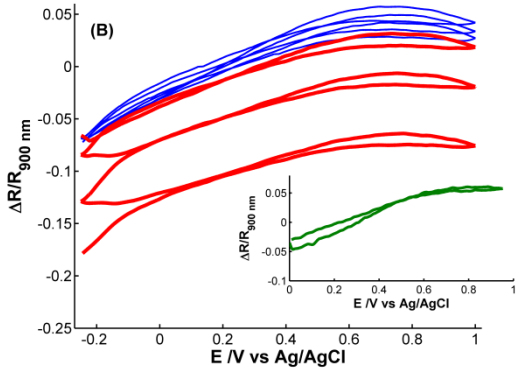

Fig4

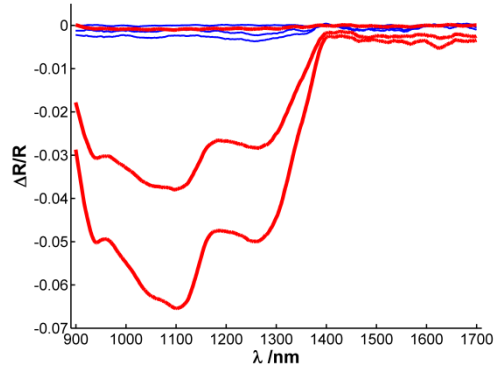

Fig5A

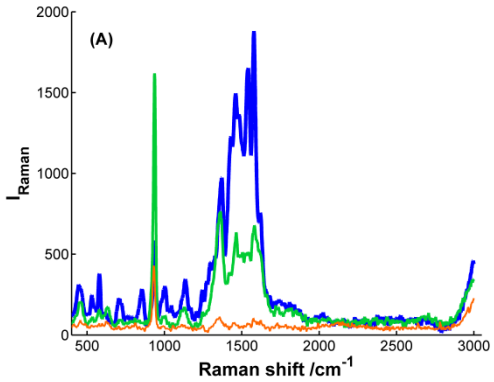

Fig5B

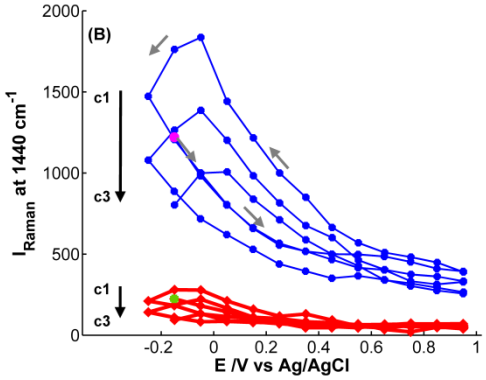

Fig6A

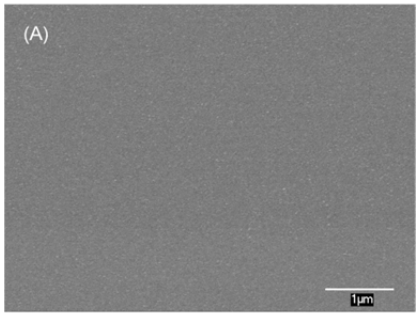

Fig6B

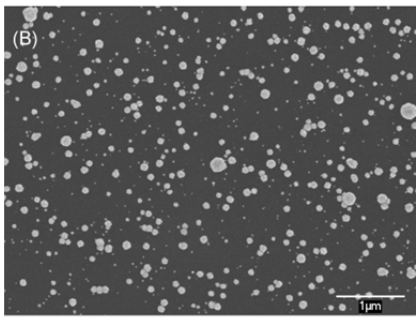

Fig7

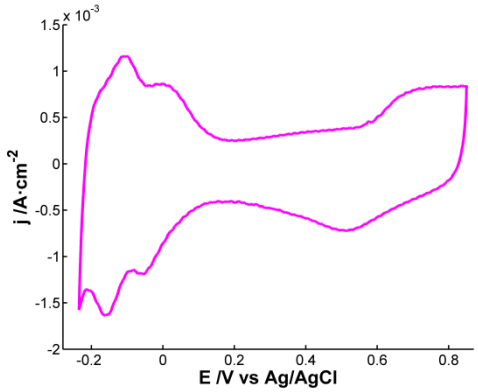

Fig8